

Modeling the reaction mechanisms for redox regulation of protein tyrosine phosphatase 1B activity

Ning Liu · Russell J. Boyd

Received: 6 December 2006 / Accepted: 21 March 2007 / Published online: 19 June 2007
© Springer-Verlag 2007

Abstract Protein tyrosine phosphatase 1B (PTP1B) functions by removing the phosphoryl group from tyrosinephosphorylated proteins in insulin signaling and metabolism. The regeneration of the active site involves a sulphenylamide intermediate derived from the intrastrand cross-linking between the catalytic serine and the neighboring backbone nitrogen. Two mechanisms have been proposed for the formation of the sulphenylamide intermediate and the subsequent reactivation of the catalytic site. In the current work, the proposed mechanisms have been investigated by the use of density functional theory calculations. Our results suggest that these two mechanisms have similar overall energy barriers and that the preferred route will be determined by the availability of hydrogen peroxide or other oxidizing reagents.

1 Introduction

Protein tyrosine phosphatases (PTPs) are enzymes that are critical to the regulation of many cellular processes, particularly in response to extracellular signals [1,2]. These enzymes remove the phosphoryl group from tyrosinephosphorylated proteins and, together with protein-tyrosine kinases, modulate the cellular level of protein-tyrosine phosphorylation (Fig. 1) [3,4]. In PTPs, a phosphate group is hydrolyzed catalytically from a tyrosine side chain, while in kinases, a phosphate is added to the side chain. A proper level and timing of tyrosine phosphorylation is critical for regulating cell growth,

differentiation, metabolism, and progression through the cell cycle, as well as cell-to-cell communication and cell death versus survival [5,6]. Genetic and biochemical studies indicate that many of these PTPs are also involved in a number of human diseases [7–9], which may be partially due to the fact that every PTP has a unique environment that brings a low pK_a to the catalytic cysteine [10].

PTPs constitute a large family of enzymes. In fact, there are about 100 PTPs encoded in the human genome [11, 12], including both cytosolic and membrane-bound receptor enzymes [5,13]. The different subfamilies are diverse in sequence, molecular weight, and specificity, but there is considerable experimental evidence that PTPs exhibit a common mechanism with related structural features.

Protein tyrosine phosphatase 1B (PTP1B) is a particular PTP whose function in insulin signaling and metabolism has been well established [14,15]. It has been observed that mice lacking PTP1B exhibit resistance to diabetes and do not develop diet-induced obesity [16,17], suggesting that PTP1B inhibitors may address both insulin and obesity resistance. PTP1B can be inactivated when exposed to reactive oxygen species such as hydrogen peroxide and superoxide [18] and therefore an insulin-stimulated burst of hydrogen peroxide can inactivate PTP1B and lead to an increase in phosphorylation levels of relevant substrate proteins. The active form of the catalytic site can be regained through the inactive protein reacting with the cellular thiol glutathione once hydrogen peroxide is diminished [19]. Recent X-ray crystallographic studies of the redox regulation of PTP1B indicate that an intrastrand protein cross-linking between the catalytic cysteine residue and a neighboring amide nitrogen [20,21] is derived from the oxidative inactivation of the enzyme. Different reaction mechanisms have been proposed to explain the formation of this 3-isothiazolidinone heterocycle and subsequent reactivation of the catalytic site (Fig. 2) [22].

Contribution to the Serafin Fraga Memorial Issue.

N. Liu · R. J. Boyd (✉)
Department of Chemistry, Dalhousie University, Halifax,
NS, Canada, B3H 4J3
e-mail: russell.boyd@dal.ca

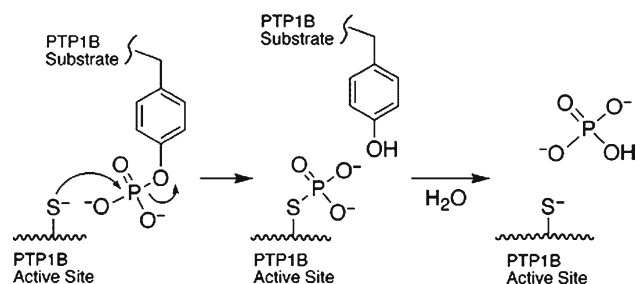


Fig. 1 Reaction catalyzed by protein tyrosine phosphatases

In the putative mechanism, the catalytic cysteine of PTP1B (E–SH) is oxidized to a sulphenic acid (E–S–OH), denoted as intermediate **2**. In the next step, the sulphenylamide (intermediate **4**) may be formed by a direct mechanism or an oxidative mechanism. In the direct mechanism, the backbone nitrogen of the neighboring serine attacks the S atom of the catalytic cysteine to yield the sulphenylamide directly with subsequent release of water. In the oxidative mechanism, intermediate **2** is further oxidized by hydrogen peroxide to form intermediate **3**, which then reacts to give the sulphenylamide. Because the nitrogen atoms of amide groups are generally considered to be poor nucleophiles, the sulphenic acid in intermediate **2** must possess sufficient electrophilicity to facilitate the attack by nitrogen of the neighboring amide. Intermediate **5**, the inactive form of the catalytic site, is derived from the sulphenylamide, through a ring-opening process. When intermediate **5** is attacked by a thiol the original form of the catalytic site is regained.

In the present work, quantum chemical calculations are carried out to study the reactivation of the catalytic cysteine in the PTP1B active site and to evaluate the proposed reaction mechanisms. A simplified model, as shown in Fig. 3, is chosen in this study to represent the active site of PTP1B.

2 Computational methods

All geometry optimizations and frequency calculations were performed with the B3LYP hybrid density functional in conjunction with the 6-31G(d) basis set by use of the Onsager reaction field method with water as the solvent at the B3LYP/6-31G(d) level [denoted Onsager-B3LYP/6-31G(d)]. The Gaussian 03 suite of programs [23] was used to perform all the calculations. Intrinsic reaction coordinate (IRC) calculations were performed on every transition state to confirm that the transition states connect the minima of interest.

In order to obtain a better estimate of the effect of solvation on the potential energy surface, single point calculations at the B3LYP/6-311++G(2df,2p) level using the conductor-like polarized continuum solvent model (CPCM) [denoted CPCM-B3LYP/6-311++G(2df,2p)] were carried out on the

geometries obtained from the Onsager-B3LYP/6-31G(d) geometry optimizations. The thermochemical energy corrections obtained from the Onsager-B3LYP/6-31G(d) frequency calculations are included in the calculations of the relative energies in water, i.e., CPCM-B3LYP/6-311++G(2df,2p)//Onsager-B3LYP/6-31G(d)+Onsager-ZPVE. Entropy contributions to the free energies of solvation at 298.15 K were derived from Onsager-B3LYP/6-31G(d) frequency calculations. All energies are in kJ/mol.

Previous studies have demonstrated the utility of the aforementioned computational methods for the study of catalysis in models of biological systems [24–27].

3 Results and discussion

1 → 2

In the first reaction step (Fig. 4), the active site of the enzyme is attacked by a hydrogen peroxide molecule, which interacts with the thiol group of the active site through a water molecule and the complex $1 \cdots (\text{H}_2\text{O}_2 + \text{H}_2\text{O})$ is formed. The complex lies 76.5 kJ/mol above the isolated system $1 + \text{H}_2\text{O}_2 + \text{H}_2\text{O}$. The reaction proceeds through transition state **TS1-2**, which has a relative energy of 178.4 kJ/mol.

The transition state is a six-membered ring formed between the thiol group of the active site, the water molecule and the attacking hydrogen peroxide. Following the transition state, another complex, $2 \cdots 2\text{H}_2\text{O}$, is formed in which the thiol group has been oxidized into the sulphenic acid (E–S–OH), lying 137.0 kJ/mol lower than the reactants. The isolated system $2 + 2\text{H}_2\text{O}$ has a relative energy of –185.6 kJ/mol.

2 → 3

The newly formed sulphenic acid (E–S–OH) intermediate **2** is oxidized further to the sulphenoperoxoic acid (E–S–OOH) intermediate **3** by hydrogen peroxide. As shown in Fig. 5, one oxygen atom of H_2O_2 interacts with the –OH of intermediate **2** through a water bridge to yield a complex $2 \cdots (\text{H}_2\text{O} + \text{H}_2\text{O}_2)$, with an energy 83.2 kJ/mol higher than that of the isolated system $2 + \text{H}_2\text{O} + \text{H}_2\text{O}_2$. Transition state **TS2-3** contains a six-membered ring, in which the other oxygen atom of the hydrogen peroxide is coordinated to the oxygen of the sulphenic acid group. The transition state lies 246.0 kJ/mol higher than the isolated system $2 + \text{H}_2\text{O} + \text{H}_2\text{O}_2$. Following the transition state, another complex $3 \cdots 2\text{H}_2\text{O}$ is formed with a relative energy of 42.8 kJ/mol. In this complex, two water molecules and the hydroxyl group of the newly formed sulphenoperoxoic acid form a loose six-membered ring via hydrogen bonding. Intermediate **3** is formed after the release of the two water molecules. The isolated system $3 + 2\text{H}_2\text{O}$ lies 5.9 kJ/mol above $2 + \text{H}_2\text{O} + \text{H}_2\text{O}_2$.

Fig. 2 Putative mechanism of 3-isothiazolidinon formation and subsequent reactivation of the catalytic site of PTP1B

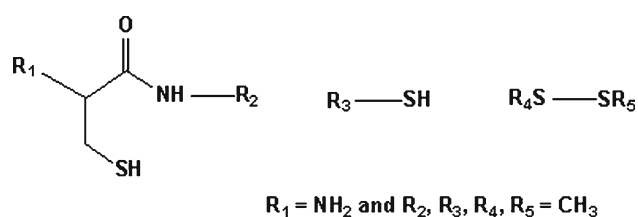
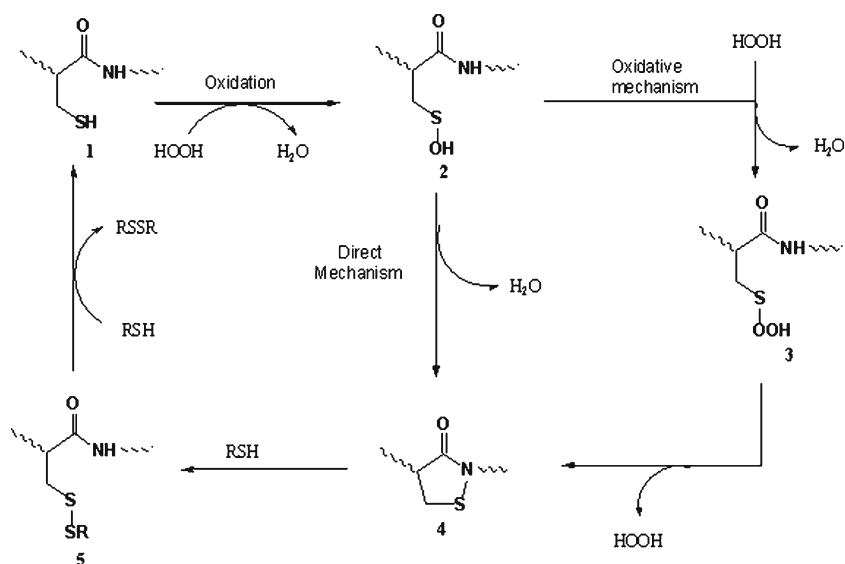


Fig. 3 A simplified model that represents the active site of PTP1B and compounds involved in the reactivation

3 → 4

In the reaction from **3** to **4** (Fig. 6), the neighboring amide nitrogen atom attacks the sulphenoperoxy acid at the *S* position, and an isothiazolidine ring is formed, with the hydrogen peroxide acting as a leaving group. Initially, a water molecule is coordinated to the compound, forming two hydrogen bonds, one between the oxygen of the water molecule and the hydrogen of the neighboring N–H, and the other between the hydrogen of the water molecule and the oxygen directly bonded to the *S* atom. The complex **3**···*H*₂O lies 3.2 kJ/mol above the isolated system **3** + *H*₂O. In the transition state **TS3-4**, the neighboring nitrogen attacks the *S* atom and a six-membered ring is formed. In this process, the water molecule donates one hydrogen atom to the –OOH group and accepts one from the nitrogen. The relative energy of **TS3-4** is 240.4 kJ/mol. Once the N–S bond is formed, the N–H and S–O bonds are completely broken. The released *H*₂O and *H*₂O₂ together with the amino group of the cysteine residue and the neighboring carboxylic group form a complex **4**···(*H*₂O₂ + *H*₂O) with a relative energy of 8.4 kJ/mol. Intermediate **4** is formed when *H*₂O and *H*₂O₂ are released. The isolated system of **4** + *H*₂O + *H*₂O₂ has an energy 45.0 kJ/mol lower than that of **3** + *H*₂O.

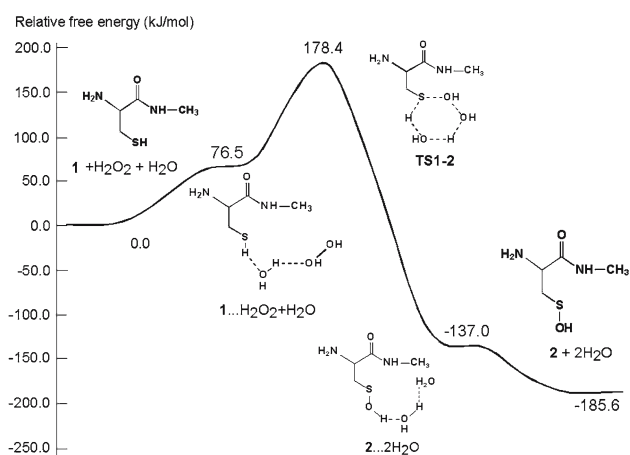


Fig. 4 Schematic free energy profile at 298.15 K for the route **1**→**2**

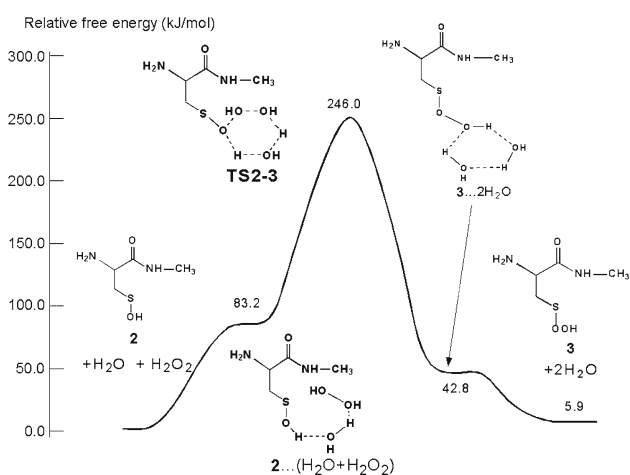


Fig. 5 Schematic free energy profile at 298.15 K for the route **2**→**3**

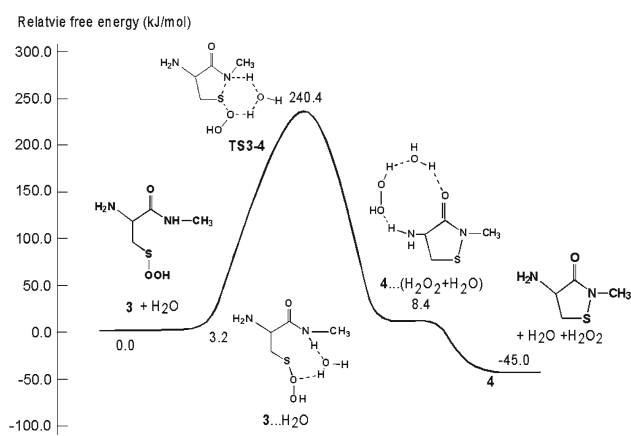


Fig. 6 Schematic free energy profile at 298.15 K for the route $3 \rightarrow 4$

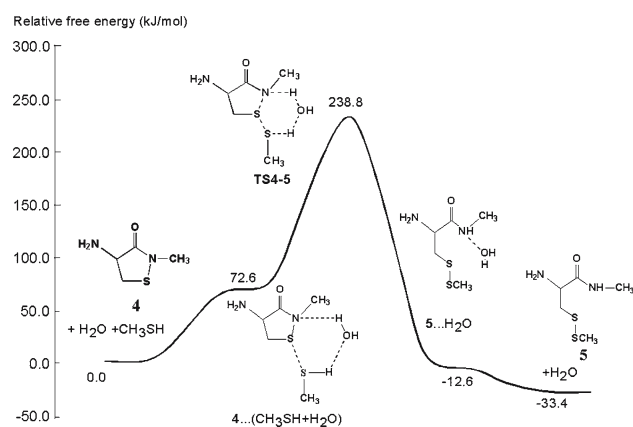


Fig. 8 Schematic free energy profile at 298.15 K for the route $4 \rightarrow 5$

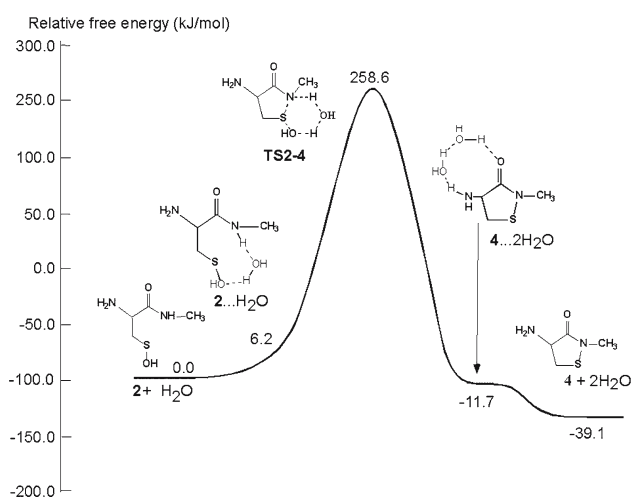


Fig. 7 Schematic free energy profile at 298.15 K for the route $2 \rightarrow 4$

$2 \rightarrow 4$

The neighboring nitrogen directly attacks the *S* of the sulphenic acid group to form intermediate **4**, which contains a five-membered isothiazolidine ring, in the reaction step $2 \rightarrow 4$ (Fig. 7). In the complex $2 \cdots \text{H}_2\text{O}$ formed before the transition state, a water molecule coordinates to the hydrogen of the neighboring N–H group and the oxygen of the sulphenic acid group through a hydrogen bond. $2 \cdots \text{H}_2\text{O}$ lies 6.2 kJ/mol above the isolated system $2 + \text{H}_2\text{O}$. A six-membered ring is formed in the transition state **TS2-4** in which the hydrogen is transferred from nitrogen to the oxygen of the sulphenic acid group and the N–S bond is formed. The relative energy of the transition state **TS2-4** is 258.6 kJ/mol. Another complex, $4 \cdots 2\text{H}_2\text{O}$, is formed after the transition state with a relative energy of –11.7 kJ/mol. The relative energy of the isolated products, $4 + 2\text{H}_2\text{O}$, is –39.1 kJ/mol.

$4 \rightarrow 5$

In the reaction $4 \rightarrow 5$ (Fig. 8), the N–S bond is broken and the inactive form, intermediate **5**, is derived. In the complex

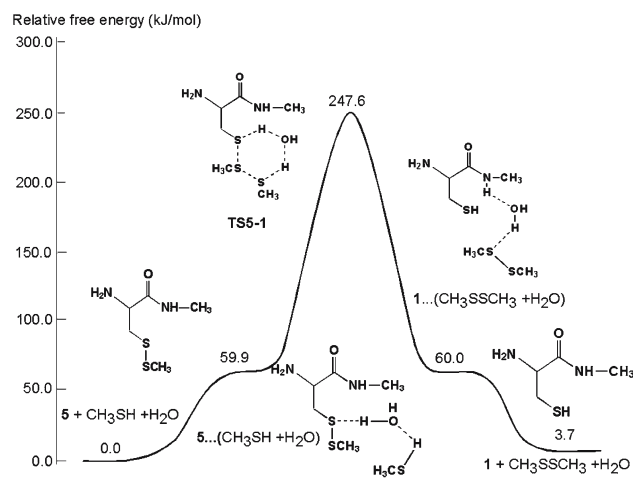


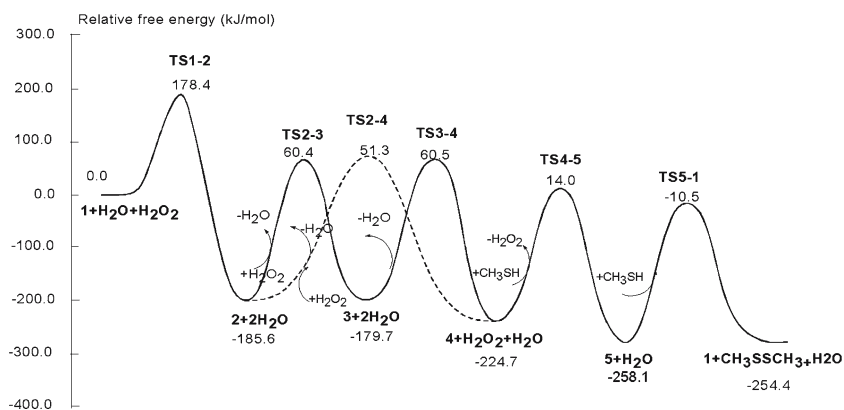
Fig. 9 Schematic free energy profile at 298.15 K for the route $5 \rightarrow 1$

$4 \cdots (\text{CH}_3\text{SH} + \text{H}_2\text{O})$, a water molecule acts as a bridge between methanethiol and the nitrogen through hydrogen bonds. Complex $4 \cdots (\text{CH}_3\text{SH} + \text{H}_2\text{O})$ lies 72.6 kJ/mol higher than the isolated system, $4 + \text{CH}_3\text{SH} + \text{H}_2\text{O}$. The transition state **TS4-5** is formed with an energy 238.8 kJ/mol higher than that of $4 + \text{CH}_3\text{SH} + \text{H}_2\text{O}$. In the transition state, a hydrogen is transferred from the methanethiol group to the neighboring nitrogen through a water bridge, the N–S bond is broken and the two *S* atoms are bonded. Another complex, $5 \cdots \text{H}_2\text{O}$, is formed after the transition state with relative energy of –12.6 kJ/mol. The relative energy of isolated system, $5 + \text{H}_2\text{O}$, is –33.4 kJ/mol.

$5 \rightarrow 1$

In this last step of the reaction loop (Fig. 9), the active site is regenerated. Initially, CH_3SH attacks the enzyme model and the complex $5 \cdots (\text{CH}_3\text{SH} + \text{H}_2\text{O})$ is formed with an energy 59.9 kJ/mol higher than that of the reactants. In the transition state, **TS5-1**, which has a relative energy of 247.6 kJ/mol, a six-membered ring is formed. A proton is transferred from the attacking CH_3SH to the *S* of the active

Fig. 10 Schematic free energy profile at 298.15 K in solution for the overall reaction (The light characters in the graph denote compounds that enter or leave the system in each reaction step)



site via a water bridge and a S–S bond is formed between the two CH₃S– groups. Another complex $1 \cdots (\text{CH}_3\text{SSCH}_3 + \text{H}_2\text{O})$ is formed after the transition state with a relative energy of 60.0 kJ/mol. Finally, the active form of the enzyme is regained in the isolated system $1 + \text{CH}_3\text{SSCH}_3 + \text{H}_2\text{O}$, which has a relative energy of 3.7 kJ/mol.

The current study involves the redox regulation of cysteine-dependent protein tyrosine phosphatases with a simplified model of the system. A sulphenylamide is formed in the transformation from the active form to the inactive form of the enzyme. Two mechanisms have been proposed to describe how sulphenylamide is derived from intermediate **2**. In the oxidative mechanism, a further oxidation step is needed to form intermediate **3** and then the backbone N in **3** attacks the S atom, leading to the formation of intermediate **4**, the sulphenylamide. In the direct mechanism, the nucleophilic attack by nitrogen leads directly to intermediate **4**.

Figure 10 gives the overall energy profile of the reaction loop. If we take the energy barrier as the energy difference between the transition state and the complex formed right before it, then the energy barriers for reaction steps $1 \rightarrow 2$, $2 \rightarrow 3$, $3 \rightarrow 4$, $2 \rightarrow 4$, $4 \rightarrow 5$ and $5 \rightarrow 1$ would be 101.9, 162.9, 237.2, 252.4, 166.2, and 187.7 kJ/mol, respectively. In the first reaction step $1 \rightarrow 2$, the energy drops by 185.6 kJ/mol, indicating that this reaction step is thermodynamically favorable. The energy barrier of reaction step $2 \rightarrow 3$ is about 90 kJ/mol lower than that of $2 \rightarrow 4$. Comparison of the energy barriers of reaction step $2 \rightarrow 4$ and $3 \rightarrow 4$ shows that they are relatively similar in magnitude. Although the energy barrier of step $3 \rightarrow 4$ is slightly bigger than that of $2 \rightarrow 4$, the difference is not significant, thus making $2 \rightarrow 4$ and $2 \rightarrow 3 \rightarrow 4$ two competitive reaction routes. When the oxidizing agent is abundant, intermediate **2** may be oxidized into **3**, and then proceed to form **4**. However, if H₂O₂ is not readily available, nucleophilic attack of the neighboring N at the S may take place to form intermediate **4**. If a thiol compound is available, the reaction may continue to yield intermediate **5**, the inactive form. Additionally, **5** can undergo reduction to give the active form of the site and complete the whole reaction loop.

Although $5 + \text{H}_2\text{O} + \text{CH}_3\text{SH}$ and $1 + 2\text{H}_2\text{O} + \text{RSSR}$ are very close to each other in energy, the newly formed RSSR is at a much lower concentration compared to the other compounds present in the system, such as water and hydrogen peroxide, and therefore the direct conversion of **1** to **5** is very unlikely to take place in vivo. In the first reaction step $1 \rightarrow 2$, one water and one hydrogen peroxide come into the system and two waters are released; in the second reaction step $2 \rightarrow 3$, one water and one hydrogen peroxide are involved and two waters are released at the end of the reaction; in the next reaction step $3 \rightarrow 4$, one water enters the system and one water and one hydrogen peroxide leave the system in the end; in the reaction step $4 \rightarrow 5$, one water and one methanethiol are added into the system and one water leaves after the reaction; in the last reaction step $5 \rightarrow 1$, one methanethiol and one water take part in the reaction and one disulfide compound and one water leave in the end. The net results are that one hydrogen peroxide and two thiol compounds are converted into two water molecules and a disulfide compound and that the total energy goes down by 254.4 kJ/mol, indicating that the reaction is irreversible.

The calculated energy barriers of step $2 \rightarrow 4$ and step $3 \rightarrow 4$ are both over 200 kJ/mol. These high energy barriers are due to the particular complex structures formed in the transition states. For example, in step $2 \rightarrow 4$ a five-membered ring and a six-membered ring are formed in the transition state, and share one S–N bond. While not stabilized by aromaticity, the transition state has a relatively high energy that arises from the distortion of the molecular plane. Similar reasoning also applies to the relatively high energy in the TS3-4. Two factors may help to lower the energy barriers of these two reaction steps: the first one is to include other active site residues into the computational model; another one is to change the structure of the transition state, namely to change the number of water molecules that are involved in proton transfer.

By comparing the structures of TS2-4 and TS3-4, it is apparent that the only difference between them is that a hydroxyl group is coordinated to the O next to the S atom

in **TS3-4** and this hydroxyl group is replaced by a hydrogen atom in **TS2-4**. Given the positions of the hydroxyl group and hydrogen in these two transition states, it is not surprising that they do not stabilize significantly the six-membered rings. Therefore, replacing the hydroxyl group in **TS3-4** by a hydrogen atom in **TS2-4** does not change the relative energy by much, as demonstrated in the current results.

Based on the above analysis, it is reasonable to believe that by either including more active site residues into the computational model or increasing the number of water molecules in the model, the energy barriers of these two mechanisms will change by a similar magnitude and the two energy barriers will still be close to each other. This suggestion is based on the similarity of the structures of transition states **TS2-4** and **TS3-4**.

4 Conclusions

The proposed competitive mechanisms for the reactivation of the catalytic cysteine in the PTP1B active site were investigated using the B3LYP method of density functional theory. The present results indicate that the efficiency of the nucleophilic attack of the neighboring nitrogen at the *S* atom is not affected by the additional oxidation that takes place at the –SOH group and therefore the oxidative mechanism and direct mechanism are competitive with each other. Whether the oxidative mechanism has priority over the direct mechanism or not should therefore depend on the availability of the oxidizing agent H₂O₂. Additionally, due to its downhill nature, the conversion reaction is predicted to be irreversible.

Acknowledgment We gratefully acknowledge the Natural Sciences and Engineering Research Council of Canada for financial support. We thank Dr. Fuqiang Ban and Jason Pearson for helpful suggestions and discussions.

References

1. Kharitonov A, Chen Z, Sures I, Wang H, Schilling J, Ullrich A (1997) *Nature* 386:181
2. Morinville A, Maysinger D, Shaver A (1998) *Trends Pharmacol Sci* 19:452
3. Tonks NK, Neel BG (2001) *Curr Opin Cell Biol* 13:182
4. Hunter T (1998) *Philos Trans R Soc Lond B Biol Sci* 353:583
5. Jackson MD, Denu JM (2001) *Chem Rev* 101:2313
6. Zhang ZY (2003) *Acc Chem Res* 36:385
7. Ren JM, Li PM, Zhang WR, Sweet LJ, Cline G, Shulman GI, Livingston JN, Goldstein BJ (1998) *Diabetes* 47:493
8. Minassian BA, Lee JR, Herbrick JA, Huizenga J, Soder S, Mungall AJ, Dunham I, Gardner R, Fong CG, Carpenter S, Jardim L, Satishchandra P, Andermann E, Snead OC III, Lopes-Cendes I, Tsui LC, Delgado-Escueta AV, Rouleau GA, Scherer SW (1998) *Nature Genetics* 20:171
9. Zhang ZY (2001) *Curr Opin Chem Bio* 5:416
10. Barford D, Das AK, Egloff MP (1998) *Annu Rev Biophys Biomol Struct* 27:133
11. Alonso A, Sasin J, Bottini N, Friedberg I, Friedberg I, Osterman A, Godzik A, Hunter T, Dixon J, Mustelin T (2004) *Cell* 117:699
12. Wang WQ, Sun JP, Zhang ZY (2003) *Curr Topics Med Chem* 3:739
13. Kennelly PJ (2001) *Chem Rev* 101:2291
14. Denu JM, Tanner KG (1998) *Biochemistry* 37:5633
15. Johnson TO, Schulman FY, Lipscomb TP, Yantis LD (2002) *Vet Pathol* 39:452
16. Elchebly M, Payette P, Michaliszyn E, Cromlish W, Collins S, Loy AL, Normandin D, Cheng A, Himms-Hagen J, Chan CC, Ramachandran C, Gresser MJ, Tremblay ML, Kennedy BP (1999) *Science* 283:1544
17. Klaman LD, Boss O, Peroni OD, Kim JK, Martino JL, Zabolotny JM, Moghal N, Lubkin M, Kim YB, Sharpe AH, Stricker-Krongrad A, Shulman GI, Neel BG, Kahn BB (2000) *Mol Cell Biol* 20:5479
18. Denu JM, Tanner KG (1998) *Biochemistry* 37:5633
19. Downes CP, Walker S, McConnachie G, Lindsay Y, Batty IH, Leslie NR (2004) *Biochem Soc Trans* 32:338
20. Salmeen A, Andersen JN, Myers MP, Tonks NK, Barford D (2000) *Mol Cell* 6:1401
21. van Montfort RLM, Congreve M, Tisi D, Carr R, Jhoti H (2003) *Nature* 423:773
22. Sivaramakrishnan S, Keerthi K, Gates Kent SJ (2005) *J Am Chem Soc* 127:10830
23. Frisch MJ, Trucks GW, Schlegel HB, Scuseria GE, Robb MA, Cheeseman JR, Montgomery JA Jr, Vreven T, Kudin KN, Burant JC, Millam JM, Iyengar SS, Tomasi J, Barone V, Mennucci B, Cossi M, Scalmani G, Rega N, Petersson GA, Nakatsuji H, Hada M, Ehara M, Toyota K, Fukuda R, Hasegawa J, Ishida M, Nakajima T, Honda Y, Kitao O, Nakai H, Klene M, Li X, Knox JE, Hratchian HP, Cross JB, Adamo C, Jaramillo J, Gomperts R, Stratmann RE, Yazyev O, Austin AJ, Cammi R, Pomelli C, Ochterski JW, Ayala PY, Morokuma K, Voth GA, Salvador P, Dannenberg JJ, Zakrzewski VG, Dapprich S, Daniels AD, Strain MC, Farkas O, Malick DK, Rabuck AD, Raghavachari K, Foresman JB, Ortiz JV, Cui Q, Baboul AG, Clifford S, Cioslowski J, Stefanov BB, Liu G, Liashenko A, Piskorz P, Komaromi I, Martin RL, Fox DJ, Keith T, Al-Laham MA, Peng CY, Nanayakkara A, Challacombe M, Gill PMW, Johnson B, Chen W, Wong MW, Gonzalez C, Pople JA (2003) *Gaussian 03, Revision B.05*. Gaussian, Inc.:Pittsburgh
24. Ban F, Rankin KN, Gauld JW, Boyd RJ (2002) *Theor Chem Acta* 108:1
25. Wu Z, Ban F, Boyd RJ (2003) *J Am Chem Soc* 125:3642
26. Wu Z, Ban F, Boyd RJ (2003) *J Am Chem Soc* 125:6994
27. Liu N, Ban F, Boyd RJ (2006) *J Phys Chem A* 110:9908